Effect of power frequency excitation character on ferroresonance in neutral-grounded system

Hui Meng(惠 萌)† and Liu Chong-Xin(刘崇新)

School of Electrical Engineering, Xi'an Jiaotong University, Xi'an 710049, *China*

(Received 11 January 2010; revised manuscript received 1 June 2010)

In most earlier ferroresonance studies the traditional excitation characteristic of iron core, in which the traditional excitation characteristic contains harmonic voltages or currents, has been used as if it were made up of pure fundamental voltage or current. However, this is not always true. In comparison with traditional excitation characteristics, this paper introduces the power frequency excitation characteristic of the iron core, which contains no harmonics. The power frequency excitation characteristic of iron core has been obtained by Elector Magnetic Transient Program, resulting in discrete voltage and current pairs. Extensive simulations are carried out to analyse the effect of power frequency excitation characteristic on potential transformer ferroresonance. A detailed analysis of simulation results demonstrates that with power frequency excitation characteristic of iron core inclusion at certain excitation voltage the ferroresonance may happen, conversely it may not happen with traditional excitation characteristic inclusion.

Keywords: ferroresonance, power frequency excitation characteristic

PACC: 0545, 0547

1. Introduction

Ferroresonance is a common phenomenon on power systems and a subject of intense study. At neutral-grounded substations, ferroresonance may happen upon switching a circuit breaker or disconnector, due to the saturated magnetizing characteristics of the bus potential transformer (PT). When ferroresonance happens, excessive voltage and current may result in a disaster such as the flashover of external insulation, burning out of PTs or destruction of the metal-oxide resistors. In the last few years the number of ferroresonance incidents has increased[1−3] and these incidents cause the power cut and destruction of PTs.

Ferroresonance is a complicated nonlinear phenomenon, which is caused by magnetic saturation of the nonlinear inductance. However, the nonlinear inductances on power systems are mainly contributed to by power transformers and inductive PTs. Under normal conditions, a nonlinear inductance operates in the linear region of its excitation characteristic. Nevertheless, when an electromagnetic transient is triggered the inductance may be forced to operate in the saturated region of its excitation characteristic. Semlyen describes the development of a Noton equivalent circuit which represents the transformer magnetizing branch in harmonic power-flow studies in Ref. [4]. In terms of these studies a method to model the magnetizing characteristic of the PT is presented. When we use this method the PT may model as a resistor parallel with a nonlinear inductance.[5] This model of PT is widely used in the ferroresonance studies afterwards.[6−10] However, the Semlyen model just represents the traditional excitation characteristic (TEC) of the PT iron core, it contains harmonic voltages and currents.

Statistics shows that among the three types of ferroresonance (fundamental, subharmonic, and harmonic), the fundamental ferroresonance (FF) occurs with the highest frequency.[11] The FF not only occurs with the highest frequency, but also involves the highest voltage and current, and leads to the severest of consequences. Nevertheless, the simulation results reveal that when the TEC model is used at certain excitation, ferroresonance does not happen, actually FF occurs in the system. This wrong judgment may result in the severest of consequences. In Refs. [11]–[13] a simple, yet effective simulation solution to FF is presented. Reference [12] has introduced the power frequency excitation characteristic (PEC) of nonlinear inductors which shows a significantly higher accuracy in the saturated region in comparison with the TEC. This paper uses the simulation solution to investigate

†Corresponding author. E-mail: xmwswws@163.com

© 2010 Chinese Physical Society and IOP Publishing Ltd

the different chaotic behaviours of a PT in a neutral-grounded 110-kV substation between TEC and PEC inclusion.

2. Theoretical analysis

2.1. Substation diagram

Ferroresonance occurs at a neutral-grounded 110-kV substation. The substation is fed by two 110-KV overhead line. A one-line diagram of the substation prone to ferroresonance is shown in Fig. 1.[13] The CB0, CB1, and CB2 represent the circuit breakers equipped with grading capacitors, and PT1 and PT2 are the single-phase electromagnetic PTs on bus sections BUS1 and BUS2, respectively. The VT1 and VT2 are the voltage transformers (VTs). All the switches named DS are the disconnect switch.

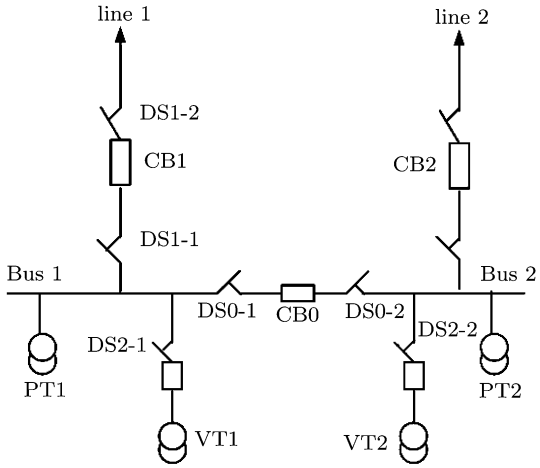


Fig. 1. Typical ferroresonance circuit.

While circuit breakers either CB0 or CB1 opens and the disconnectors DS0-1, DS0-2, DS1-1, DS1-2 are closed, ferroresonance will happen if the other one opens. Furthermore, when any one of the four disconnectors opens, ferroresonance will happen again. Likewise, it is probable that the ferroresonance will happen the third time if the open disconnector turns closed. Because the disconnector DS2-1 is opened, the VTs are not in the ferroresonant circuit during the ferroresonance. Figure 2 depicts Thevenin equivalent circuit of Fig. 1. In this study the PT is modeled by a nonlinear flux-controlled inductance L_2 and the nonlinear resistance R_2 represents core loss of PT. Furthermore, R_1 and L_1 represent the resistance and leakage inductance of primary winding. The C is Thevenin equivalent capacitance of grading capacitance of circuit breaker and phase to ground capacitance.

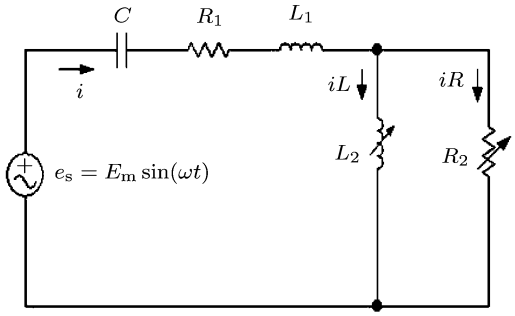


Fig. 2. Thevenin equivalent circuit of Fig. 1.

2.2. TEC and PEC of PT

In this paper the example PT is a JCC2-110 potential transformer. It is installed on the bus bar of a 110-kV substation where ferroresonance was frequently stimulated. The JCC2-110 PT is of 0.5 class, has a rated capacity of 500 VA, and a turns ratio $n = 110000/\sqrt{3} : 100/\sqrt{3} = 1100$. The TEC of the PT was measured on its secondary with a circuit the same as that shown in Fig. 3(a). The voltage and current values were listed in Table 1.[13] The PEC of the PT was simulated by EMTP software and the circuit shown in Fig. 3(b). The voltage and current were listed in Table 2.[13] Where $U_{\rm T}$ and $I_{\rm T}$ present the TEC of the PT, likewise, $U_{\rm P}$ and $I_{\rm P}$ present the PEC of the PT.

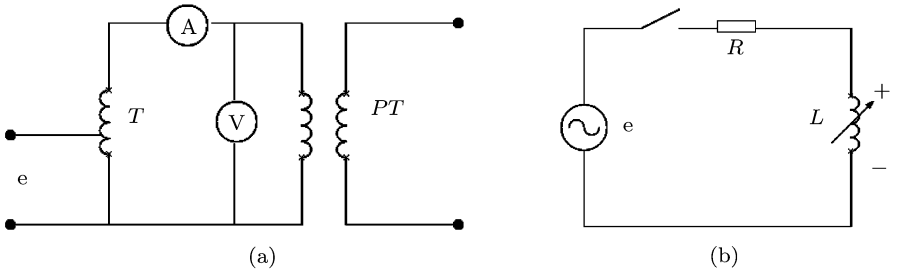


Fig. 3. Circuit of measuring (a)TEC, (b) PEC.

Table 1. The TEC of PT.

$U_{\rm T}$/V	56.6	62.8	66.6	69.9	74.0	78.3	82.1	85.5
$I_{\rm T}$/A	1.25	2.00	3.00	4.10	6.00	8.00	10.0	12.0

Table 2. The PEC of PT.

$U_{\rm P}$/V	55.0	64.5	70.7	78.5	85.6	99.0	111	126
$I_{\rm P}$/A	1.22	2.45	3.95	6.94	9.83	22.5	37.1	55.0

By using a tool such as SATURA, a supporting subroutine embedded in EMTP, the U–I data shown in Tables 1 and 2 could be converted into a φ–i curve, where φ is the magnetic flux in the inductor and i is the current flowing through it. The φ–i data converted by SATURA shown in Tables 3 and 4 and figure 4 is the relevant φ–i curve. In Fig. 4 the φ–i data are all in p.u value (per unit quantity).

Table 3. The φ–i data of TEC.

$\varphi_{\rm T}$/V.s	0.089	0.179	0.282	0.300	0.333	0.370	0.409
$I_{\rm T}$/A	0.608	1.21	3.98	6.46	12.86	19.91	32.47

Table 4. The φ–i data of PEC.

$\varphi_{\rm P}$/V.s	0.248	0.290	0.318	0.353	0.385	0.446	0.500
$I_{\rm P}$/A	1.73	4.80	7.94	13.90	18.68	45.71	71.16

The dashed line in Fig. 4 is the flux–current curve of PT's PEC and the solid line is the flux–current curve of PT's TEC. It can be found that in the linear region the two lines are almost superposition; this means that under the normal working condition the TEC of PT is the same as PEC of PT. However, in the nonlinear region the nonlinear inductance is driven into magnetic saturation. Because the current flowing through the inductor contains harmonics, we make the PEC curve higher than the corresponding TEC curve. This difference could cause the different results whether the system is working normally.

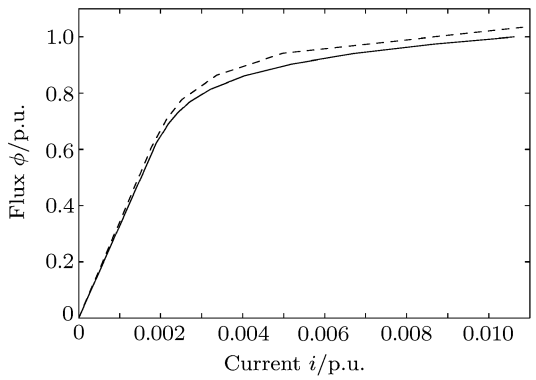


Fig. 4. The φ–i curve of PT in p.u. (per unit quantity).

2.3. System modeling

The Thevenin equivalent circuit of the system is shown in Fig. 2. In terms of the inclusion given by Ref. [6], the core loss of PT shown in Fig. 2 is

$$i_{R_2} = h_0 + h_1 V_{R_2} + h_2 V_{R_2}^2 + h_3 V_{R_2}^3, \tag{1}$$

the parameters are $h_0 = -3.5213 \times 10^{-3}$, $h_1 = 5.7869 \times 10^{-7}$, $h_2 = -1.4167 \times 10^{-12}$, $h_3 = 1.21105 \times 10^{-18}$.

While the nonlinear inductance L_2 is driven into saturation region where the flux–current curve is fitted by a polynomial[4,7]

$$i_L = a\varphi + b\varphi^n, \tag{2}$$

where φ denotes the flux in the nonlinear inductance L_2 and in terms of the study shown in Ref. [14] the exponent $n = 11$. While considering the TEC of PT, the coefficients $a = 0.0030$, $b = 0.0076$. Likewise, while considering the PEC, the coefficients $a = 0.0029$, $b = 0.0044$.

The differential equations for this circuit are

$$V_{R_2} = \frac{{\rm d}\varphi}{{\rm d}t}, \tag{3}$$

$$i = a\varphi + b\varphi^n + h_0 + h_1 V_{R_2} + h_2 V_{R_2}^2 + h_3 V_{R_2}^3, \tag{4}$$

$$E_{\rm m}\sin(\omega t) = u_{\rm c} + R_1 i + L_1 \frac{{\rm d}i}{{\rm d}t} + V_{R_2}, \tag{5}$$

$$C\frac{{\rm d}u_{\rm c}}{{\rm d}t} = i. \tag{6}$$

Taking $x = \varphi$, $y = {\rm d}\varphi/{\rm d}t$, $z = u_{\rm c}$ as state variables and substituting these state variables into Eqs. (3)–(6) we obtain

$$\frac{\mathrm{d}x}{dt} = y, \tag{7}$$

$$\frac{\mathrm{d}y}{\mathrm{d}t} = \frac{E_{\mathrm{m}}\sin(\omega t) - z - y - R_1(ax + bx^n + h_0 + h_1 y + h_2 y^2 + h_3 y^3) - L_1(ay + nbx^{n-1} y)}{L_1(h_1 + 2h_2 y + 3h_3 y^2)}, \tag{8}$$

$$\frac{\mathrm{d}z}{\mathrm{d}t} = \frac{ax + bx^n + h_0 + h_1 y + h_2 y^2 + h_3 y^3}{C}, \tag{9}$$

where φ is flux in inductance L_2 in p.u value, ω is the power frequency of 1.0 p.u value.

3. Simulation results and discussion

In this paper the effects of PEC and TEC of PT on the ferroresonance in power system are discussed. The simulation study is carried out based on this point. Bifurcation diagrams, Poincare maps and phase–plane diagrams are three main means to distinguish between various modes of behaviour. Furthermore, the Lyapunov exponent is also used to distinguish chaos from steady state. For solving the system of differential equations, the Matlab environment and an embedded package of fourth-order Runge–Kutta method were used. Figures 5 and 6 are the bifurcation diagrams of the effect of varying the magnitude of the source voltage on the chaotic behaviour of TEC and PEC. The initial conditions taken for simulation are $\omega = 1$, $E_{\mathrm{m}} = 1$, $x = 0$, $y = 1.065$, $z = 1.55$ in p.u value. The varying parameter is the magnitude of source voltage E_{m}. Several cases and combinations have been investigated, however, only the representative ones are presented here.

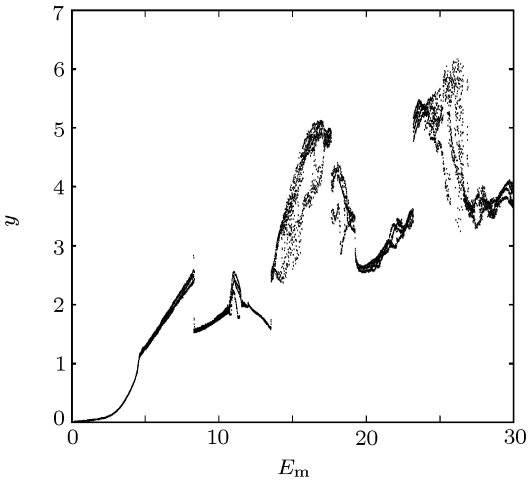


Fig. 5. Bifurcation diagram for TEC of PT.

To classify the effects of varying source voltage E_{m} of Eqs. (7)–(9) on the behaviour of the system shown in Fig. 2, extensive simulations have been carried out. In order to predict which kind of ferroresonance may occur for a wide range of magnitude of source voltage change, we obtain the bifurcation diagram by changing i_L between TEC and PEC. Figure 5 shows the bifurcation diagram for considering TEC of PT, figure 6 shows the bifurcation diagram for considering PEC of PT. Varying parameter is the magnitude of source voltage. Parameter at Y-axis is the voltage on the core loss R_2.

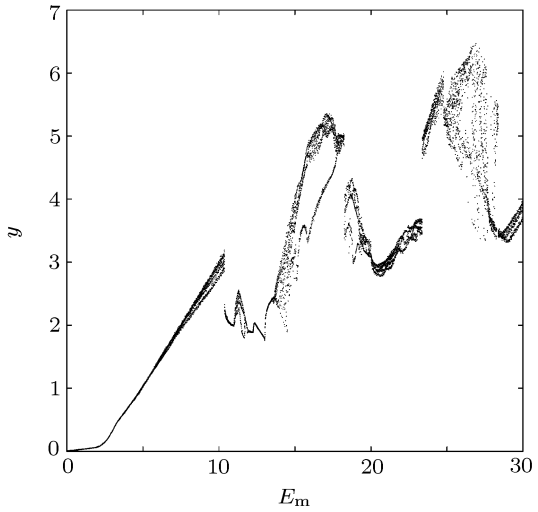


Fig. 6. Bifurcation diagram for PEC of PT.

The bifurcation diagrams shown in Figs. 5 and 6 reveal what modes of ferroresonance are possible for a given excitation. The single-value area of the bifurcation map indicates one period, dual-value indicates two periods, etc. The tendency of ferroresonance mode changes in Fig. 6 is semblable as Fig. 5, this reveals that FF is a major factor in the ferroresonance. One characteristic precursor to chaotic motion is the appearance of sub-harmonics. There exists a transitional region from periodic road to chaos. In the transitional region the waveform of V_{R_2} is still periodic but not a sinusoidal one as the source voltage and the trajectory in phase–plane is changing from limit cycle to strange attractors. It could be found that the transitional region is started at $E_{\mathrm{m}} = 5$ p.u in Fig. 5, however, the inflexion in Fig. 6 is at almost $E_{\mathrm{m}} = 3$ p.u. Consequently, with PEC considered the system is driven into subharmonic resonance earlier than that with TEC considered. The region with

many scattered points which looks blurred in Figs. 5 and 6 indicates chaotic ferroresonance. There are clear differences between Figs. 5 and 6 in the chaotic ferroresonance. When the excitation voltage is in certain interval, the system is driven into chaotic ferroresonance with PEC considered, however, it is not with TEC considered.

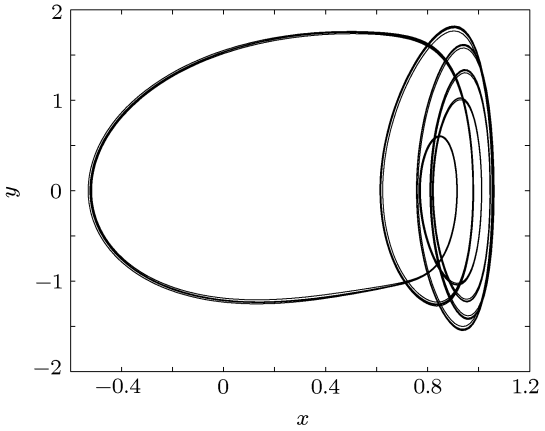


Fig. 7. Phase plane orbit of $E_{\rm m} = 10$ p.u with TEC.

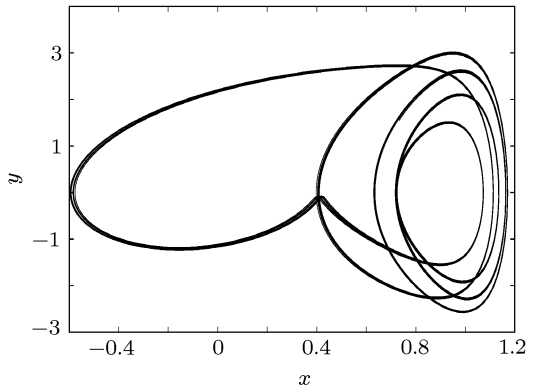


Fig. 8. Phase plane orbit of $E_{\rm m} = 10$ p.u with PEC.

It can be observed from these figures that the V_{R_2} voltage jumping phenomena happen at all these two figures. For example, the corresponding excitation is $E_{\rm m} = 8.2, 14$ p.u in Fig. 5, at $E_{\rm m} = 10, 14$ p.u in Fig. 6. While these phenomena happen, the voltage of V_{R_2} in Fig. 6 is higher than that in Fig. 5, but the extent of voltage jump is almost the same. Figures 7 and 8 show the phase plane orbit of $E_{\rm m} = 10$ p.u, where the voltage jumping phenomena happen. The sharp corner of the phase plane orbit in Fig. 8 shows the jumping phenomena while PEC is considered. However, the phase plane orbit is smooth while TEC is considered in Fig. 7.

As the analysis in Subsection 2.1, because the current flowing through the inductor contains harmonics, which makes the PEC curve higher than the corresponding TEC curve. This difference will lead different results whether the chaotic ferroresonance happens in the system at certain excitation voltage such as $E_{\rm m} = 11.7$. Figure 9 shows the phase plane orbit and Poincare map while $E_{\rm m} = 11.7$ with PEC considered. The corresponding maximum Lyapunov exponents are calculated to be $\sigma = 0.0241$. The positive Lyapunov exponent means that the ferroresonance is driven into chaos, and the phase plane orbit is a strange attractor. The points shown in Poincare map (Fig. 9(b)) are random and unsystematic. This indicates that the system has changed through periodicity to chaos. Nevertheless, when we consider TEC, the corresponding maximum Lyapunov exponents of Fig. 10 are calculated to be $\sigma = -0.0340$. The phase plane orbit shown in Fig. 10(a) is a periodical orbit and Poincare map is a series of regular dots distributed in Fig. 10(b) while the excitation $E_{\rm m} = 11.7$ p.u. The negative Lyapunov exponent and Poincare map mean that the system is stable.

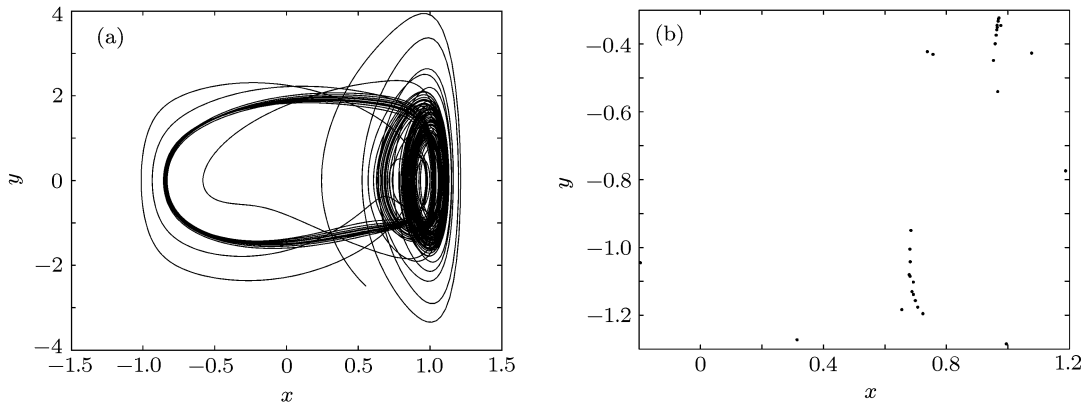


Fig. 9. (a) Phase plane orbit. (b) Poincare map of $E_{\rm m} = 11.7$ with TEC.

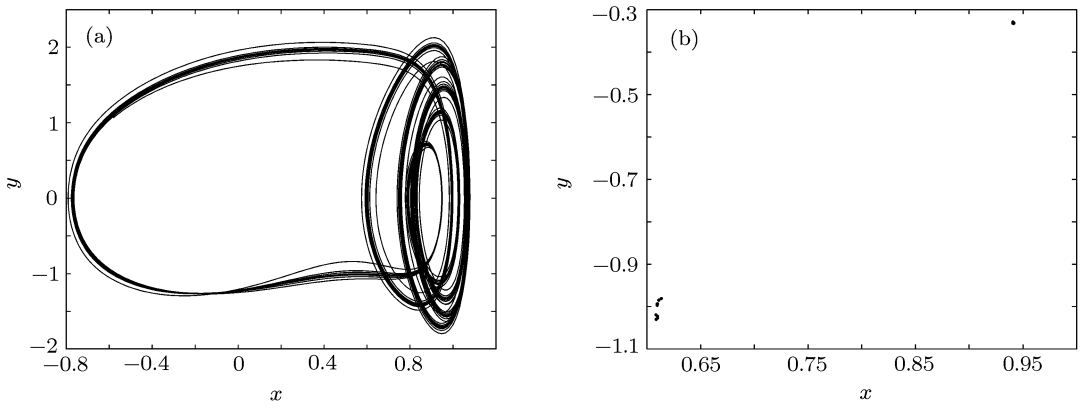


Fig. 10. (a) Phase plane orbit. (b) Poincare map of $E_{\rm m} = 11.7$ with PEC.

4. Conclusions

This paper shows some obtained results of investigating the influence of PEC on the behaviour of a neutral-grounded substation in power system. The main conclusions drawn from this study are: i) fundamental ferroresonance is a major factor in the ferroresonance; ii) with the PEC the ferroresonance model is optimistic than that with TEC considered; iii) the fundamental ferroresonance may start at certain excitation with PEC but it does not happen with TEC considered. Considering the PEC of PT, we find that the ferroresonance model may become more exact, the ferroresonance accidents may reduce to a lower level.

References

[1] Ta P T and Chia C N 2006 *IEEE Trans. Power Delivery* **21** 1006
[2] Shen Y H and Zhi X 2008 *QingHai Electric Power* **27** 48 (in Chinese)
[3] Zhang L 2008 *East China Electric Power* **36** 148 (in Chinese)
[4] Semlyen A, Acha E and Arrillaga J 1987 *IEE Proc-C* **134** 162
[5] Marti J R and Soudack A C 1991 *IEE Proc-C* **138** 321
[6] Hui M, Zhang Y B and Liu C X 2009 *Chin. Phys.* B **18** 1787
[7] Araujo A E A, Soudack A C and Marti J R 1993 *IEE Proceedings-C* **110** 237
[8] Alona B T, Vivien K and Graeme W 2001 *IEEE Trans. Power Delivery* **16** 205
[9] Al-Anbarri K, Ramanujam R, Subba C H and Kuppusamy R K 2003 *Electric Power Systems Research* **65** 1
[10] Si-Ma W X, Liu F, Sun C X, Liao R J and Yang Q 2006 *Acta Phys. Sin.* **55** 5714 (in Chinese)
[11] Li Y G, Shi W and Li F R 2006 *IEEE Trans. Power Delivery* **21** 788
[12] Li Y G, Shi W and Li F R 2006 *IEEE Trans. Power Delivery* **21** 794
[13] Li Y G 2004 *Ph.D. Dissertation*, School Elec. Eng., Xi'an Jiaotong University, Xi'an, China
[14] Hui M, Zhang Y B and Liu C X 2008 *Chin. Phys.* B **17** 3258